Photofission cross section of ^{232}Th

H. X. Zhang, T. R. Yeh,* and H. Lancman
Physics Department, Brooklyn College of the City University of New York, Brooklyn, New York 11210
(Received 23 December 1985; revised manuscript received 16 June 1986)

The photofission cross section of ^{232}Th was measured in the 5.8–12 MeV energy range with an average photon energy resolution of 600 eV. Intermediate structure was observed at 5.91, 5.97, and 6.31 MeV. The experimental fission probability and various properties of the intermediate structure were compared with calculated values based on a double-humped fission barrier as well as a triple-humped one. The results favor, though not decisively, the presence of a shallow third well in the barrier. Certain features of both barriers, a rather high first hump and a deep secondary well, are quite different from those predicted by current theoretical barrier calculations.

I. INTRODUCTION

Since the discovery of the double-humped fission barrier in actinide nuclei, extensive experimental and theoretical work has been done on various aspects of fission.[1] Of great value have been experimental investigations at excitation energies in the vicinity of the barrier because of the information they supply on the details of its character and shape. Very fruitful in this respect have been experiments on particle transfer reactions leading to fission[2,3] as well as experimental studies of neutron-induced fission.[1] The latter in particular, because of their characteristically high neutron energy resolution, proved to be an excellent tool for investigating the complex level structure at sub-barrier excitation energies. As a result of these efforts, the main features of the fission barrier are now well understood.

Persisting interest in the fission of thorium isotopes has been caused in part by the difficulty in resolving the question of the existence of a theoretically predicted third minimum in their fission barriers.[1,4] The most direct evidence in favor of such a complex barrier has been provided by the observation[5] of rather narrow resonances in neutron-induced fission of ^{231}Th and ^{233}Th. Fine structure observed within these resonances in high resolution measurements has been interpreted as corresponding to rotational bands built on undamped vibrational states. Various features of this structure appear to be in support of a triple-humped barrier with an inner barrier *A* considerably lower than barriers *B* and *C*. However, it has been shown by Lynn[6] that the observed structure could also result from coupling of single particle and vibrational motion in these nuclei.

In ^{232}Th, whose barrier is also expected[4,7,8] to be triple-humped, sub-barrier excitation energies are not accessible in neutron-induced fission because the neutron separation energy is higher than the barrier. Such energies, however, can be reached in photofission. Accurate photofission measurements are best done with monochromatic gamma rays of variable energy. Such measurements have been done on ^{232}Th at $E_\gamma < 8$ MeV by Dickey and Axel,[9] and by Knowles *et al.*,[10] with tagged bremsstrahlung having an energy resolution of 70 keV and 13 keV, respectively. In both cases the photofission cross section exhibits structure, the most prominent manifestation of which is a broad resonance at 6 MeV. We recently[11] reported results of measurements of the photofission cross section of ^{232}Th at excitation energies close to the top of the barrier. The necessary photons were derived from (p,γ) resonances in several light nuclei. They had an energy resolution better than 500 eV. These measurements revealed resonances resulting from compound states in the second well of the barrier (intermediate structure). Various properties of this structure could be understood within the framework of the double-humped barrier, although the possibility of a shallow third minimum could not be excluded.

Although the details of the shape of the fission barrier are reflected most directly in the behavior of the fission cross section at excitation energies in the vicinity of the barrier, measurements at higher photon energies also provide useful information. Such measurements are also important for the understanding of the fission decay of the giant quadrupole resonance.[12,13] Existing data have been obtained using quasimonochromatic photons from annihilation of positrons in flight. The energy resolution of such photons is 250 keV. Cross sections obtained by Veyssiere *et al.*[14] for several actinide nuclei are in substantial disagreement with the more recent results of Caldwell *et al.*[15] In the case of ^{232}Th, the results of the two experiments differ by about 30% on the average. Recently reported measurements by Ries *et al.*[16] on ^{235}U and ^{238}U involving counting of fission fragments instead of neutrons as in the two other experiments, appear to confirm the values reported for these two nuclei by Veyssiere. However, results of Arruda-Neto *et al.*[13] obtained with continuous bremsstrahlung are in better agreement with the data of Caldwell.

The aim of the present measurements was to continue the investigations of intermediate structure over a wider energy range than the one reported earlier,[11] and to extend the cross section measurements to higher energies in order to resolve the existing discrepancy between the published values of the cross sections. Preliminary results of this work have been described before.[17]

II. EXPERIMENTAL SETUP AND PROCEDURES

The (p,γ) resonances chosen for these experiments are characterized by small natural width, large gamma ray yield, and decay by emission of only, or predominantly, one gamma ray with an energy higher than 5 MeV. Since the lifetime of a typical resonance is considerably shorter than the average stopping time of the recoiling compound nucleus in the material of the target, the energy of the emitted gamma ray is fully Doppler-shifted. It varies with the angle of emission θ relative to the proton beam (see Fig. 1) according to the expression

$$E_\gamma = E_0[1+(v/c)\cos\theta] ,$$

where v is the velocity of the recoiling nucleus. A typical value of $dE_\gamma/d\theta$ is 300 eV/deg at $\theta=90°$, and a typical photon energy range is 20 keV.

Since high proton beam currents, 150 μA on the average, have to be used in order to ensure an adequate photon flux, a target chamber designed[18] to withstand the large beam power dissipation was employed. The target materials were deposited on a water-cooled thin Ta foil. The foil, mounted at the end of a bellows, vibrated in two mutually perpendicular directions in the plane perpendicular to the proton beam, spreading the beam over a large target area. High vacuum was maintained in the chamber to prevent deposit of contaminations on the target. In choosing the target materials, care was taken to avoid isotopes with (p,n) thresholds below the proton energy for the particular (p,γ) resonance. Each Ta foil was thoroughly cleaned and repeatedly heated in vacuum before the target was deposited.

The experimental setup was the same as the one described before.[11,17] Foils of thorium, 30 mg/cm^2 thick, containing 99.9% of ^{232}Th were sandwiched between 8 μm thick strips of polycarbonate film (Kimfol). The sandwiches were located on a cylindrical surface coaxial with the proton beam (Fig. 1) which was provided by the Brooklyn College Dynamitron accelerator. The Kimfol film served as the fission fragment track detector. In order to determine the gamma ray intensity and spectrum, a large, efficiency calibrated, Ge(Li) detector (not shown) was placed at 90° to the proton beam.

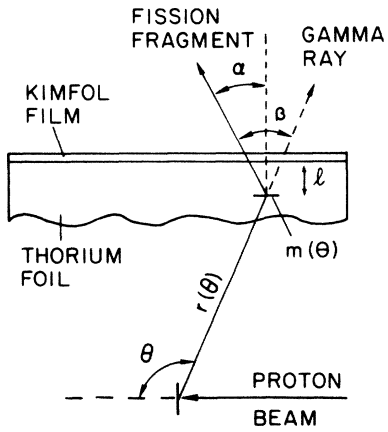

FIG. 1. Part of the fission fragment detection setup showing a fragment emitted from depth 1 in the thorium foil. The sandwiches of Kimfol film and thorium foil are located on a cylindrical surface coaxial with the proton beam.

To make the handling of the sandwiches manageable, the thorium foil was cut into 5 cm$\times$5 cm squares. Each square was covered by a 100 μg/cm^2 layer of gold on both sides to protect its surface from oxidation. It was necessary to use 90 such squares to ensure an adequate counting rate of the fission fragments.

The efficiency calibration of the Kimfol film for counting the thorium fission fragments, and the procedures used in developing the film were described elsewhere.[19] The scanning of the developed film for fission fragment tracks was done with a high-resolution vidicon camera. A detailed description of the setup used for scanning was also given elsewhere.[20]

III. DATA REDUCTION

In the cylindrical geometry used here, fission fragments produced by photons of energies between E_γ and $E_\gamma+\Delta E_\gamma$ are created in strips of foil defined by the intersections of the cylindrically shaped foil with cones of vertex angles θ and $\theta+\Delta\theta$ originating at the proton target (see Fig. 1).

The photofission cross section $\sigma_{\gamma f}$ at photon energy E_γ is related to the fission fragment counts $N(E_\gamma)$ in a strip of width $m(\theta)$ corresponding to an energy interval ΔE_γ by the expression

$$N(E_\gamma)=\frac{2I(\theta)}{4\pi r^2(\theta)}\sigma_{\gamma f}(E_\gamma)nLm(\theta)\eta(\theta) . \quad (1)$$

Here $I(\theta)=IW(\theta)R(\theta)$ is the intensity of the gamma rays at angle θ, I is the intensity of the photons coming from the proton target, $W(\theta)$ is the photon angular distribution function and $R(\theta)$ accounts for absorption of the photons on their way to the strip, n is the number of target nuclei per unit volume, L is the length of the strip, $r(\theta)$ is its distance from the photon source, and

$$\eta(\theta)=\int\int\int F(\beta)\Omega(1,\alpha)\sin\beta\, d\beta\, d\phi\, d1 , \quad (2)$$

where $F(\beta)$ accounts for the angular distribution of the fission fragments[21] relative to the direction of the gamma rays, and $\Omega(1,\alpha)$ is the efficiency of the Kimfol film[19] for detecting fragments emitted from depth 1 in the foil at an angle α to the normal. The angles θ, α, β, and the azimuthal angle ϕ are related by

$$\cos\alpha=\cos\beta\sin\theta-\cos\theta\sin\beta\sin\phi . \quad (3)$$

The photofission cross section is found for each energy E_γ by adding the numbers of tracks counted in strips found at angle θ in all Kimfol films. In plotting the cross section versus the photon energy, the choice of the energy interval per channel ΔE_γ was dictated by the total number of accumulated counts at a given (p,γ) resonance and by the photon energy resolution.

IV. RESULTS AND DISCUSSION

A. The photofission cross section

The photofission cross sections obtained with gamma rays from several (p,γ) resonances are shown in Fig. 2. The target isotope and proton resonance energy are indicated in each case. Twenty-two such spectra were taken in the photon energy range from 5.8 to 12 MeV. The average duration of each run was 20 h. The statistical accuracy of the counts, shown by the error bars, varies from spectrum to spectrum, reflecting the fluctuation of the strength of the (p,γ) resonances.

The photon energy resolution depends on several factors. Among them are the angular photon energy dispersion, the accuracy of the alignment of the films relative to the proton beam, the accuracy of the determination of the track position,[20] and the natural width of the (p,γ) resonances. In cases where the last contribution is negligible, the energy resolution ranges from 200 eV for the lower photon and resonance proton energies and heavier (p,γ) target isotopes, to 700 eV for the high photon and proton energies and light target isotopes.

The cross sections averaged over the photon energy range at each (p,γ) resonance are plotted versus the average photon energy in Fig. 3, where data reported previously[11] have been included. Two adjacent spectra at 6.17 MeV are represented by one point. The error bars include counting errors (negligible), errors in the efficiency calibration of the gamma ray and fission fragment detectors, uncertainties in the angular distribution of the fission fragments and the gamma rays, and uncertainties in the alignment of the thorium foils and Kimfol films relative to the proton target. The plotted cross sections were corrected for contributions caused by the unwanted gamma rays emitted from some (p,γ) resonances. Except for

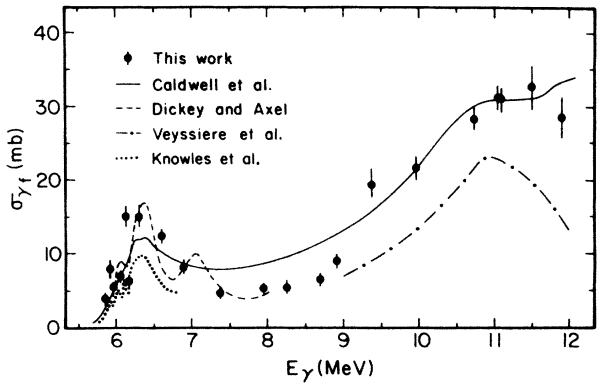

FIG. 3. Photofission cross sections obtained in different experiments. The results of this work are averaged over the photon energy range at each (p,γ) resonance.

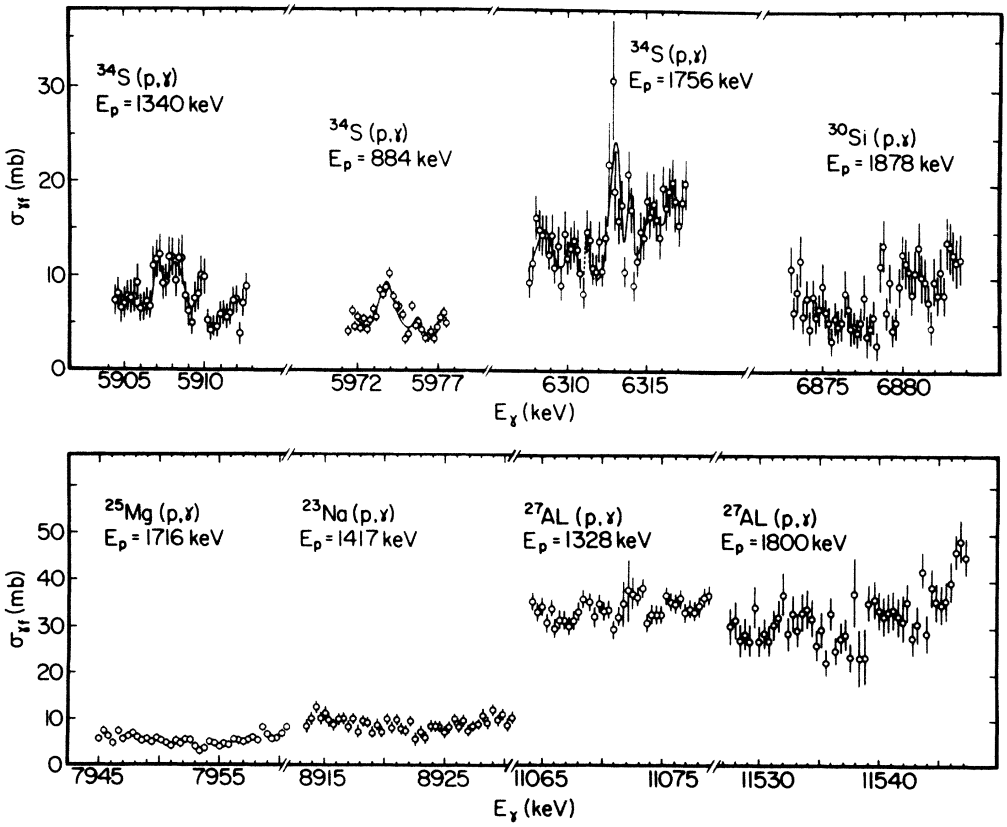

FIG. 2. Photofission cross section of ^{232}Th for several photon energies. The (p,γ) resonances used to produce the photons and the resonance proton energies are listed in each case. The average photon energy resolution in the three spectra exhibiting structure is 300 eV.

one case, these corrections did not exceed 10% of the presented values. The sum of the contributions from fission caused by neutrons from (γ,n), $(\gamma,2n)$, and fission, as well as the contribution from (γ,nf), were estimated to be smaller than 2%.

Our results are in good agreement with those of Dickey and Axel,[9] and at energies above 9 MeV, those of Caldwell *et al.*[15] They are systematically higher than the results of Knowles *et al.*[10] They are also higher than the cross sections reported by Veyssiere *et al.*[14] The broad resonance at 6 MeV, clearly seen in the data of Knowles and Dickey, has been confirmed by $(p,p'f)$ measurements.[22] It should be kept in mind while comparing the various data that our results are obtained by averaging over an energy interval at least an order of magnitude smaller than in the other experiments.

B. The fission probability

The fission probability is obtained by dividing the measured photofission cross section by the total gamma-ray absorption cross section σ_γ. Thus $P_f=\sigma_{\gamma f}/\sigma_\gamma$. This quantity is shown in Fig. 4 vs the gamma ray energy. It is assumed that fission occurs at the excitation energy $E=E_\gamma$. The values of σ_γ were taken directly from Ref. 15 for photon energies higher than 9 MeV. Below this energy they were obtained by extrapolation.[15] The calculated fission probability that provides the best fit to the data up to the $(\gamma,2n)$ threshold is shown by the solid line. It was computed using the program FISSAL developed for a double-humped fission barrier by Back and Britt.[24] The statistical model on which the program is based is discussed in detail by Back *et al.*[2] We therefore describe it here only briefly.

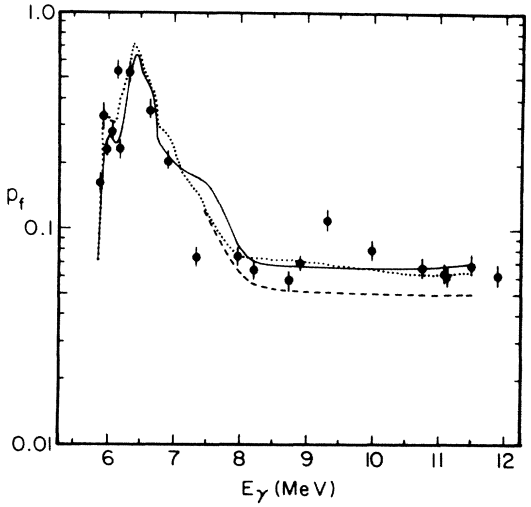

FIG. 4. Comparison of the fission probability of ^{232}Th with the results of calculations based on the statistical model. The solid line is for axially asymmetric, reflection symmetric barrier *A* and axially symmetric, reflection asymmetric barrier *B*. The dashed line is computed assuming axial symmetry, reflection asymmetry for both barriers. The dotted line is based on the same assumption as the dashed one but with $E_B^{0^+}$ lower by 200 keV.

The fission probability is given in its usual form

$$P_f(E)=\sum_{J^\pi}\alpha(EJ^\pi)\frac{\Gamma_f(EJ^\pi)}{\Gamma_t(EJ^\pi)}S\ , \tag{4}$$

where $\alpha(EJ^\pi)$ is the probability of populating a state with spin J and parity π by photoabsorption, $\Gamma_t=\Gamma_f+\Gamma_n+\Gamma_\gamma$ is the total width of the state, and Γ_f, Γ_n, and Γ_γ are its partial widths for decay by fission, neutron emission, and gamma-ray emission, respectively. S is a correction factor for width fluctuation.[1] All widths are averaged over many states at excitation energy E. The averaging obliterates structure resulting from compound states in both wells while preserving the much wider spaced vibrational resonances in the second well.

The gamma-ray width is calculated by summing the widths for all transitions to states at lower energy in the first well, assuming that only $E1$ transitions take place. Similarly, the neutron emission width is computed by summing the transmission coefficients for transitions to all possible final states in the A-1 nucleus.

The average fission width is obtained from

$$\Gamma_f(EJ^\pi)=\frac{D_{\rm I}(EJ^\pi)}{2\pi}\sum_K T_f^K(EJ^\pi)\ , \tag{5}$$

where $D_{\rm I}$ is the average level spacing at ground state deformation, and T_f^K are the barrier penetrabilities for the transition states with different spin projections K on the nuclear symmetry axis. These penetrabilities are found analytically by solving the Schrödinger equation for a double-humped fission barrier. The barrier is formed by joining smoothly three parabolic sections which represent its two humps and the well between them (second well). Thus

$$V(\epsilon)=E_l\pm\mu\omega_l^2(\epsilon-\epsilon_l)^2/2\ ,$$

where, in the commonly used notation, $l=A$ for the first hump, B for the second, and II for the well; ϵ is the deformation parameter, $\mu=0.054A^{5/3}\hbar^2$ MeV^{-1}, and $\hbar\omega_l$ are the curvatures of the parabolas.

The penetrabilities found in this way exhibit resonances at energies of vibrational states in the second well. To account for the damping of these states into the compound states in the second well, an imaginary term is added to the potential

$$U(\epsilon)=-W(E)+C(\epsilon-\epsilon_{\rm II})^2/2\ , \tag{6}$$

where

$$W(E)=w(E-E_{\rm II}-\Delta_n-\Delta_p)+W_0\ ,$$

Δ_n and Δ_p are the neutron and proton pairing gaps, $C=4W/(a^2+b^2)$ is found from the condition that $U(a)+U(b)=0$, and a and b are the joining points of the parabolas. As a result of the addition of the imaginary term, the penetrability T_f becomes a sum of two parts

$$T_f=T_D+T_I\ , \tag{7}$$

where T_D represents direct and T_I indirect fission, i.e., fission preceded by the excitation of compound states in the second well.

Under the assumption of K mixing in the second well, when several transition states contribute to the process, the sum in Eq. (5) has to be replaced by (N_D+N_I), where $N_D=\sum_K T_D^K$, and $N_I=N_{\rm abs}N_B/(N_A+N_B)$. Here $N_{\rm abs}=\sum_K A^K$, and $N_{A,B}=\sum_K T_{A,B}^K$, where A^K is the flux absorbed in the second well from transition state K, and

$$T_{A,B}^K=\{1+\exp[2\pi(E_{A,B}^K-E)/\hbar\omega_{A,B}^K]\}^{-1}$$

are the Hill-Wheeler penetrabilities of barriers A and B for transition states K.

In the absence of damping, all $A^K=0$, whereas for complete damping, all $T_D^K=0$. The latter case is assumed in the nonresonance version of the program which is used to calculate the fission probability at energies well above the barrier. In this case the probability is decided by the density of states at barriers A and B. This density, in turn, strongly depends on the symmetry of the fissioning nucleus at the deformation of each barrier. In the present calculation, following Back *et al.*,[2] we used the resonance version of the program at energies below 7.5 MeV; above that energy, the nonresonance version was used. However, we found that between 6.5 and 7.5 MeV the results obtained with the two versions differ insignificantly. Barrier A was taken to have axial asymmetry, reflection symmetry; barrier B axial symmetry, reflection asymmetry. The population probabilities for the states reached by electric dipole and quadrapole excitations were taken to be 0.98 and 0.02, respectively,[23] independent of excitation energy.

Not all parameters defining the barrier can be uniquely determined by fitting the experimental fission probability. Fortunately, some can be found independently from other data. The value of E_{II} is determined by the density of class II states[11] at 6.16 MeV. The spacing of the resonances at 6.313 MeV, $D_{II}=1.3\pm0.3$ keV, is in excellent agreement with this value. The average areas of the observed intermediate structure set the values of $E_A^{0^-}$ and $E_B^{0^-}$ at 6.10 ± 0.2 MeV and 6.50 ± 0.2 MeV, respectively. The other parameters were varied to provide the best fit (solid line in Fig. 4). The results are compared with other determinations in Table I.

Although the overall agreement between the values of the parameters determined in different experiments is good, there are several exceptions. The values $E_A^{0^-}$ found by Van der Plicht *et al.*[25] is too high to account for the measured average areas of the class II resonances. Our data confirm their value of $E_B^{0^+}$, which is higher than the values obtained in the other experiments. Our value for $E_B^{1^-}$ is somewhat higher than the two other values; however, of these two, the value from Ref. 11 was obtained by fitting the average areas of the class II resonances, which is not very sensitive to $E_B^{1^-}$. In the present case, $E_B^{1^-}$ is determined mainly by the fission probability at 7 MeV, where the contributions of $K^\pi=1^-$ and 0^- fission become comparable. The $J^\pi=2^+$ barrier parameters cannot be determined from the present data because of the small value of $\alpha(2^+)$.

Given the theoretical prediction[4,7,8] of a rather low barrier A and a barrier B split by a third well, it is tempting to compare the calculated fission probability for such a barrier with the experimental data. If the first barrier is low, then, in order to account for the intermediate structure and the broad vibrational resonance, it is necessary to assume that the third well has a minimum at ~3 MeV. Since the low first barrier does not affect the fission probability at energies around 6 MeV, the part of the barrier which has to be considered is the double humped part comprised of barriers B and C at higher deformations. To compute the fission probability, we assume that both barriers B and C are axially symmetric and reflection asymmetric,[8] and that they are characterized by parameters listed in Table I, with $A=B$ and $B=C$. The result is shown by the dashed line in Fig. 4. Agreement with experiment at higher energies can be improved by lowering $E_B^{0^+}$ by 200 keV, which results in the dotted line. Clearly, on the basis of the present data it is impossible to choose between this barrier and the ordinary double-humped one.

C. Intermediate Structure

1. Background

The spectra in Fig. 2 at 5908, 5975, and 6313 keV exhibit structure which we interpret as representing class II compound states in the second well of the barrier. As in the cases reported previously,[11] the observed peaks are superimposed on a rather high background. Its magnitude is determined by fitting each spectrum with a function

TABLE I. Parameters of the double-humped fission barrier (in MeV).

	K^π	Ref. 22	Ref. 1	Ref. 9	Ref. 25	Ref. 2	Ref. 11	This work
	0^+	5.8	5.82	5.5	5.7	<5.5		5.82
E_A	0^-	6.75		6.3	6.7		6.15	6.10
	1^-			6.5			6.55	6.55
$\hbar\omega_A$		0.9	1.0	0.9	0.9		0.9	1.0
	0^+	6.75	6.22	6.1	6.6	6.15		6.40
E_B	0^-	6.75		6.3	6.6		6.55	6.50
	1^-			6.9			6.85	7.25
$\hbar\omega_B$		1.2	0.75	0.5	1.2	0.5	0.65	0.7
$E_{\rm II}$		3.0		3.0	3.0		2.8	2.8
$\hbar\omega_{\rm II}$		1.5		1.5	1.5			0.9
W_0		0.05			0.05			0.05
w		0.25			0.15			0.15

$$\sigma_{\gamma f}(E_\gamma)=\sigma_b(E_\gamma)+\sum_i A_i \exp[-B_i(E_\gamma-E_i)^2] , \quad (8)$$

where $\sigma_b(E_\gamma)=aE_\gamma^2+bE_\gamma+c$, and E_i are the energies of the peaks. To compare the magnitudes of σ_b with theoretical expectations, it is useful to express the cross section in terms of the fission probability.

Employing the picket-fence model for the class II compound states, we can write for the fission probability at energy $E=E_i+x$ below the (γ,n) threshold

$$P_f(x)=\sum_{J^\pi}\alpha\frac{\Gamma_f(x)+\Gamma_D}{\Gamma_f(x)+\Gamma_D+\Gamma_\gamma}S . \quad (9)$$

We will assume that $\alpha(1^-)=1.0$.

When overlap of class II compound resonance tails is not neglected, $\Gamma_f(x)$ represents the sum of contributions from all class II states to the fission width at x. This has the form[2]

$$\Gamma_f(x)=\frac{\Gamma_{IIc}\Gamma_{IIf}D_I}{\Gamma_{II}D_{II}}\times\frac{\sinh(\pi\Gamma_{II}/D_{II})}{\cosh(\pi\Gamma_{II}/D_{II})-\cos(2\pi x/D_{II})} , \quad (10)$$

where Γ_{IIc}, Γ_{IIf}, and Γ_{II} are, respectively, the coupling, fission, and total widths of the class II compound states. In the presence of several transition states K with incompletely damped vibrational resonances in the second well at energies E^K_{IIv},

$$\Gamma_{IIc,f}=\frac{D_{II}}{2\pi}\sum_K \Gamma^K_{A,B}\Gamma^K_w/[(E-E^K_{IIv})^2+(\Gamma^K_{IIv}/2)^2] , \quad (11)$$

where

$$\Gamma^K_{A,B}=\frac{\hbar\omega^K_{II}}{2\pi}T^K_{A,B} , \quad (12)$$

and Γ^K_w and Γ^K_{IIv} are, respectively, the damping and total widths of the vibrational resonances. When damping in the second well is complete

$$\Gamma_{IIc,f}=\frac{D_{II}}{2\pi}\sum_K T^K_{A,B} .$$

The direct fission width is given by the expression

$$\Gamma_D=\frac{D_I}{2\pi}\sum_K T^K_D .$$

For a double-humped fission barrier, T_D can be obtained from FISSAL, but for the purpose of computing the properties of the intermediate structure, which depend very strongly on the positions of the vibrational resonances in the second well, it is better to calculate T_D in a way that will allow us to use the experimental values of the energies of these resonances as independent input data. A suitable expression for T_D of a double-humped barrier can be derived with the aid of the Wentzel-Kramers-Brillouin (WKB) approximation. In such a derivation the loss of direct flux due to damping in the second well can be accounted for by adding to the potential the imaginary part given by Eq. (6).

According to Bhandari[30] for a potential $V(\epsilon)+iU(\epsilon)$

$$T_D=T_AT_B\exp(-2\delta)\{1+2\exp(-2\delta)[(1-T_A)(1-T_B)]^{1/2}\cos 2\nu+(1-T_A)(1-T_B)\exp(-4\delta)\}^{-1} , \quad (13)$$

where

$$\delta=-\left[\frac{\mu}{2\hbar^2}\right]^{1/2}\int_{\epsilon'}^{\epsilon''}\frac{U(\epsilon)}{[E-V(\epsilon)]^{1/2}}d\epsilon ,$$

and ϵ' and ϵ'' are the classical turning points at energy E in the second well. The phase angle ν can be determined locally from

$$\nu=\left[\frac{E-E_{IIv}}{\hbar\omega_{II}}+\frac{1}{2}\right]\pi .$$

The penetrability computed according to Eq. (13) is in good overall agreement with the one given by FISSAL.

The damping width of a resonance in the second well can be estimated from

$$\Gamma_w=\frac{\hbar\omega_{II}}{2\pi}[1-\exp(-4\delta)] .$$

In the absence of damping, i.e., when $W=0$, $\delta=0$ and no indirect fission occurs. Indeed in this case $\Gamma_f(x)=0$, as

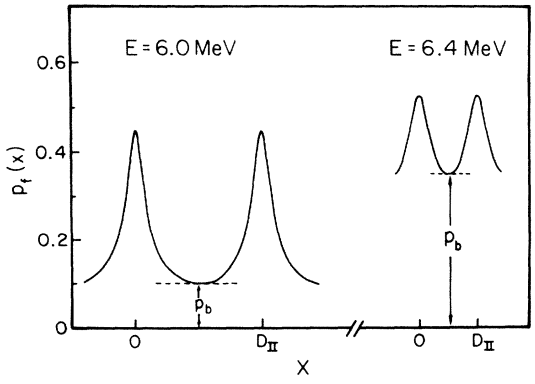

FIG. 5. Intermediate structure in the fission probability calculated at two excitation energies for the double-humped fission barrier.

TABLE II. The average areas, widths, and underlying backgrounds of the intermediate structure resonances.

E	A (b eV)			W (eV)		P_b		
(MeV)	Expt.	Calc[a]	Calc[b]	Calc[a]	Calc[b]	Expt.	Calc[a]	Calc[b]
6.313	5.2±1.7	3.3	3.2	440	440	0.34±0.07	0.35	0.41
6.175	5.1±1.7	4.2	4.9	370	420	0.16±0.03	0.21	0.24
6.144	13.0±4.0	4.2	5.0	350	430	0.25±0.05	0.19	0.34
6.074	3.1±1.5	4.6	5.0	400	470	0.18±0.05	0.19	0.15
5.975	4.8±1.6	5.0	5.2	620	550	0.12±0.02	0.13	0.12
5.908	5.4±1.5	2.4	5.4	200	310	0.24±0.05	0.035	0.21

[a]Double-humped barrier.
[b]Triple-humped barrier.

can be seen from Eqs. (10) and (11). On the other hand, when δ is very large, damping becomes complete.

It may be noted that in the vicinity of a resonance, T_D given by Eq. (13) is well approximated by a Lorentzian function of energy, whereas far from resonances it is proportional to the product $T_A T_B$. This is in general agreement with the algebraic structure of T_D used in the doorway-state model of Goldstone and Paul,[26] where the Lorentzian terms reflect coupling of the compound states in the first well to vibrational resonances in the second well, and the smoothly varying $T_A T_B$ term originates from coupling of the compound class I resonances to the completely damped vibrational resonances in the first well. The vibrational resonances act as doorways to fission.

If the barrier is assumed to be triple humped, the penetrability of barrier B in Eqs. (12) and (13) has to be replaced by the overall penetrability T_{BC} of parts B and C of the barrier, whose shapes as before are approximated by parabolic functions of deformation. For a shallow third well in which no damping takes place, T_{BC} is given by Eq. (13) in which $\delta=0$, and T_A and T_B are replaced by T_B and T_C, respectively.

To calculate $P_f(x)$, one needs to know the energies $E_{\mathrm{II}v}$ and $E_{\mathrm{III}v}$ of the vibrational resonances in the second and third well within the energy range of interest. But despite persistent efforts made in search for resonance structure in the cross section of ^{232}Th, its details are not well established. In addition to the broad resonance at 6 MeV, considerably narrower resonances have been reported by Knowles *et al.* at 5.92 and 6.11 MeV. However, the latter two resonances cannot be discerned in the spectra of Dickey and Axel taken with monochromatic photons of energy resolution 70 keV. They also do not appear in the fission cross section measured by Janszen *et al.*[22] with an energy resolution of 17 keV.

Because of these uncertainties concerning the existence of the narrow resonances we have assumed only one resonance at 6 MeV in the calculations with the double-humped barrier, whereas in the triple-hump calculations all three peaks were assumed to exist; the two narrow ones, in the third well. In order of increasing energy these peaks were taken to have $J^\pi,K=1^-,0$, 1^-0, and 1^-1. The last assignment does not contradict the results of the measurements of the angular distribution of the fission fragments.[21]

The background underlying intermediate structure can be defined as $P_b=P_f(D_{\mathrm{II}}/2)$. This is illustrated in Fig. 5, where $P_f(x)$ is plotted at two excitation energies, with only two peaks shown at each energy. P_b represents background in spectra measured with sufficiently high energy resolution. It contains contributions from direct fission and peak overlap.

The values of P_b computed at the energies where intermediate structure has been resolved in the present and previously reported[11] experiments are compared in Table II with the values of $P_b^{\mathrm{exp}}=\sigma_b/\sigma_\gamma$ averaged over each measured spectrum. For the double-humped barrier the parameters used in the calculations were taken from Table I; for the triple-humped barrier they are listed in Table III. The overall agreement between the experimental values and the calculated ones for both barrier shapes is quite good at all energies except 5908 keV, where the large value of P_b appears to confirm the existence of the narrow vibrational resonance at 5920 keV.

2. *Average resonance area*

The average area of the class II resonances that one may expect to observe directly in a spectrum is

$$A=\sigma_\gamma\int_0^{D_{\mathrm{II}}}[P_f(x)-P_b]dx\ . \tag{14}$$

This can be written in the form

$$A=\sigma_\gamma D_{\mathrm{II}}(P_2-P_1)\Gamma_\gamma/(\Gamma_\gamma+\Gamma_D)\ , \tag{15}$$

TABLE III. Parameters of the triple-humped fission barrier (in MeV).

K^π	E_A	$\hbar\omega_A$	E_B	$\hbar\omega_B$	E_C	$\hbar\omega_C$	$\hbar\omega_{\mathrm{II}}$	$\hbar\omega_{\mathrm{III}}$	W_0	w
0^-	6.2	1.0	6.25	0.37	6.3	1.2	0.9	0.9	0.05	0.10
1^-	6.55	1.0	6.30	0.4	6.7	1.2	0.9	0.9		

where

$$P_1=\frac{S\Gamma_f(x=D_{II}/2)}{\Gamma_f(x=D_{II}/2)+\Gamma_D+\Gamma_\gamma},$$

and

$$P_2=SG\{[G+\cosh(\pi\Gamma_{II}/D_{II})]^2-1\}^{-1/2},$$

with

$$G=\frac{\Gamma_{IIc}\Gamma_{IIf}D_I}{\Gamma_{II}(\Gamma_\gamma+\Gamma_D)D_{II}}\sinh(\pi\Gamma_{II}/D_{II}).$$

It can easily be verified that when $\Gamma_{II}\ll D_{II}$ and $\Gamma_D\ll\Gamma_\gamma$, the second term in Eq. (14) disappears and Eq. (15) assumes the form given for A in Ref. 11, where direct fission and overlap of class II states were neglected.

The areas obtained from Eq. (15) are compared with the average experimental resonance areas in Table II. The data reported previously, with one exception, are included in this comparison. The omitted value at 5.87 MeV was obtained with a (p,γ) resonance, which, as we have learned recently,[28] has a natural width of 1.7 keV. Therefore, the structure observed at this energy may have reflected the existence of only the strongest class II resonances. Considering the fact that the experimental average areas in Table II are based on a limited number of peaks in each spectrum, the agreement with the calculated values for both barrier shapes is good. It is, in fact, slightly better in the case of the triple-humped barrier, but given the limited amount of data the difference cannot be taken as conclusive.

From Fig. 5 and the calculated areas listed in Table II, it is clear that near the top of the barrier, intermediate structure becomes increasingly difficult to observe as the excitation energy increases.

3. *Average fission probability*

It is interesting to compare $P_f(x)$ averaged over the intermediate structure with $P_f(E)$ given by FISSAL. This is done in Fig. 6, where the averaged $P_f(x)$ is plotted for both shapes of the fission barrier. The large difference between the results of FISSAL and $P_f(x)$ obtained for a double-hump barrier below 6 MeV results from the fact that FISSAL yields a slightly lower value for the energy of the broad vibrational resonance than the measured value taken for computing $P_f(x)$. As before, the experimental points, particularly the ones at 5908 and 6140 keV, favor the triple-humped barrier.

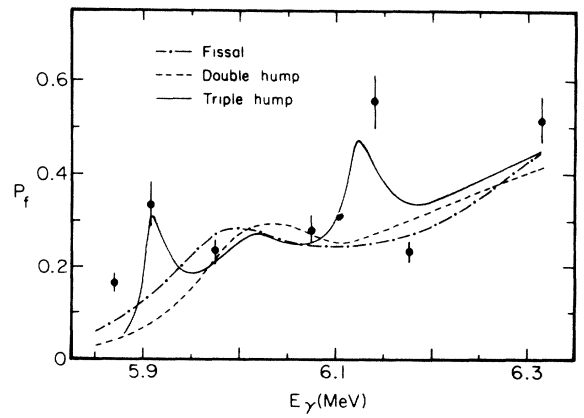

FIG. 6. The fission probability near the top of the barrier. The experimental points represent the average values at each (p,γ) resonance.

Below the energy range of Fig. 6 the cross section decreases rapidly. Data obtained in different experiments vary substantially. Knowles *et al.* reported peaks at 5.5 and 5.6 MeV each about 50 keV in width. These peaks appear to have been confirmed in the measurements done by Findlay *et al.*[31] with continuous bremsstrahlung. Within the framework of either of the present models these peaks could be understood as 1^-,0 and 1^-,1 vibrational states in the second well. The expected width of such states, due mainly to damping, is 80 keV. This identification would imply a separation of vibrational states of about 500 keV. That this is smaller than $\hbar\omega_{II}$ is not unexpected near the top of the well.[27]

Finally, it may be noted that at excitation energies well above the barrier the fission probability is not sensitive to the details of the shape of the barrier.

V. CONCLUSIONS

We have measured the photofission cross section in 21 narrow energy intervals between 5.8 and 12 MeV, with an average photon energy resolution of about 600 eV. The investigation of the intermediate structure was extended to 6.3 MeV. From studies of the properties of this structure and the dependence of the fission probability on the excitation energy, we have determined the possible values of the parameters of a double-humped and triple-humped barrier. The data confirm our previous finding that in ^{232}Th a barrier of 6 MeV is followed by a deep intermediate well with a minimum at 2.8 MeV independent of the shape of the remaining part of the barrier. This is contrary to the theoretical predictions[4,7,8] of a much lower first barrier followed by two shallow wells. Indications that the first barrier in the adjacent ^{233}Th is also considerably higher than the one predicted theoretically and that it is followed by a deep secondary well were found by Perez *et al.*[29] in their measurements of the ^{232}Th(n,f) cross section.

Because of the limited amount of data and lack of firm information concerning the gross structure of the cross section at sub-barrier excitation energies, the present results are not sufficient to determine with reasonable certainty whether a third well exists in the fission barrier of ^{232}Th, although it favors the existence of such a well. For a conclusive determination more extensive measurements of structure have to be done.

ACKNOWLEDGMENTS

We wish to thank D. King and B. Stuber for their expert maintenance of the Dynamitron during the course of these experiments. The contributions of Dr. P. X. Zhu and Dr. M. Ismail during their stay at this laboratory are gratefully acknowledged. This work was supported in part by the U.S. Department of Energy and by the Professional Staff Congress—Board of Higher Education Faculty Research Award Program of the City University of New York.

*Present address: Institute of Nuclear Energy Research, P.O. Box 3, Taiwan, Republic of China.

[1]S. Bjornholm and J. E. Lynn, Rev. Mod. Phys. **52**, 725 (1980).

[2]B. B. Back, O. Hansen, H. C. Britt, and J. D. Garrett, Phys. Rev. C **9**, 1924 (1974).

[3]P. Glassel, H. Rosler, and H. J. Specht, Nucl. Phys. **A256**, 220 (1976).

[4]P. Moller and J. R. Nix, *Proceedings of the Third International Symposium on the Physics and Chemistry of Fission, Rochester, 1973* (International Atomic Energy Agency, Vienna, 1974), Vol. 1, p. 103.

[5]J. Blons, C. Mazur, D. Paya, M. Ribrag, and H. Weigmann, Nucl. Phys. **A414**, 1 (1984).

[6]J. E. Lynn, J. Phys. G **9**, 665 (1983).

[7]J. Dudek, W. Nazarewicz, and A. Faessler, Nucl. Phys. **A412**, 61 (1984).

[8]W. M. Howard and P. Moller, At. Data Nucl. Data Tables **25**, 219 (1980).

[9]A. Dickey and P. Axel, Phys. Rev. Lett. **35**, 501 (1975).

[10]J. W. Knowles, W. F. Mills, R. N. King, B. O. Pich, S. Yen, R. Sobie, L. Watt, T. E. Drake, L. S. Cardman, and R. L. Gulbranson, Phys. Lett. **116B**, 315 (1982).

[11]H. X. Zhang, T. R. Yeh, and H. Lancman, Phys. Rev. Lett. **53**, 34 (1984).

[12]H. Stroher, R. D. Fischer, J. Drexler, K. Huber, U. Kneissl, R. Ratzek, H. Ries, W. Wilke, and H. J. Maier, Phys. Rev. Lett. **47**, 318 (1981).

[13]J. D. T. Arruda-Neto, W. Rigolon, S. B. Herdade, and H. L. Riette, Phys. Rev. C **29**, 2399 (1984).

[14]A. Veyssiere, H. Beil, R. Bergere, P. Carlos, A. Lepretre, and K. Kernbath, Nucl. Phys. **A199**, 45 (1973).

[15]J. T. Caldwell, E. J. Dowdy, B. L. Berman, R. A. Alvarez, and P. Meyer, Phys. Rev. C **21**, 1215 (1980).

[16]H. Ries, G. Mank, J. Drexler, R. Heil, K. Huber, U. Kneissl, R. Ratzek, H. Stroher, T. Weber, and W. Wilke, Phys. Rev. C **29**, 2346 (1984).

[17]T. R. Yeh, and H. Lancman, IEEE Trans. Nucl. Sci. NS-28, 1289 (1981).

[18]H. X. Zhang and H. Lancman, Nucl. Instrum. Methods A **239**, 459 (1985).

[19]T. R. Yeh and H. Lancman, Nucl. Instrum. Methods **179**, 141 (1981).

[20]H. X. Zhang, T. R. Yeh, and H. Lancman, Nucl. Instrum. Methods **214**, 391 (1983).

[21]N. S. Rabotnov, G. N. Smirenkin, A. S. Soldatov, L. N. Usachev, S. P. Kapitza, and Yu, M. Tsipenyuk, Yad. Fiz. **11**, 508 (1970) [Sov. J. of Nucl. Phys. **11**, 285 (1970)].

[22]H. Janszen, S. Brandenburg, R. DeLeo, M. N. Harakeh, B. Visscher, and A. Van der Woude, *Dynamics of Nuclear Fission and Related Collective Phenomena* (Springer Verlag, Berlin, 1981), p. 95.

[23]J. R. Huizenga and H. C. Britt, in *Proceedings of the International Conference on Photonuclear Reactions and Applications, Asilomar 1973,* edited by B. L. Berman (U.S. Atomic Energy Commission Office of Information Services, Oak Ridge, Tennessee, 1973), Vol. 2, p. 833.

[24]We wish to thank Dr. B. Back for providing us with a copy of the program.

[25]J. Van Der Plicht, M. N. Harakeh, A. Van der Woude, P. David, J. Debrus, J. Janszen, and J. Schulze, Nucl. Phys. **A369**, 51 (1981).

[26]P. Goldstone and P. Paul, Phys. Rev. C **18**, 1733 (1978).

[27]P. D. Goldstone, F. Hopkins, R. E. Malmin, and P. Paul, Phys. Rev. C **18**, 1706 (1978).

[28]G. Adams, E. G. Bilpuch, G. E. Mitchell, R. O. Nelson, and C. R. Westerfeldt, J. Phys. G **10**, 1747 (1984).

[29]R. B. Perez, G. de Saussure, J. H. Todd, T. J. Yang, and G. F. Auchampaugh, Phys. Rev. C **28**, 1635 (1983).

[30]B. S. Bhandari, Phys. Rev. C **19**, 1820 (1979).

[31]D. J. S. Findlay, G. Edwards, M. P. Hawkes, and M. R. Sene, in *Capture Gamma-Ray Spectroscopy and Related Topics—1984,* Proceedings of the International Symposium Capture Gamma-Ray Spectroscopy and Related Topics, Knoxville, Tennessee, 1984, AIP Proc. No. 125, edited by S. Raman (AIP, New York, 1985), p. 237.